An improved exponential transformation for nearly singular boundary element integrals in elasticity problems

Guizhong Xie, Jianming Zhang, Yunqiao Dong, Cheng Huang, Guangyao Li

StateK ey Laboratory of Advanced Design and Manufacturing for Vehicle Body, College of

Mechanical and Vehicle Engineering, Hunan University, Changsha 410082, China

Correspondence to: Jianming Zhang

College of Mechanical and Vehicle Engineering, Hunan University, Changsha 410082, China

Telephone: +86731-88823061

E-mail: zhangjianm@gmail.com

Abstract: This paper present an improved exponential transformation for nearly singular boundary element integrals in elasticity problems. The new transformation is less sensitive to the position of the projection point compared with the original transformation. In our work, the conventional distance function is modified into a new form in polar coordinate system. Based on the refined distance function, an improved exponential transformation is proposed in polar coordinate system. Moreover, to perform integrations on irregular elements, an adaptive integration scheme considering both the element shape and the projection point associated with the improved transformation is proposed. Furthermore, when the projection point is located outside the integration element, another nearest point is introduced to subdivide the integration elements into triangular or quadrilateral patches of good shapes. Numerical examples are presented to verify the proposed method. Results demonstrate the accuracy and efficiency of our method.

1.   introduction

Near singularities are involved in many boundary element method (BEM) analyses of engineering problems, such as problems on thin shell-like structures [Krishnasamy *et al* (1994); Liu (1998)],

the crack problems [Dirgantara (2000)], the contact problems [Aliabadi (2000)], as well as the sensitivity problems [Zhang D *et al* (1999)]. Accurate and efficient evaluation of nearly singular integrals with various kernel functions of the type $O(1/r^{\chi})$ is crucial for successful implementation of the successful implementation of the boundary type numerical methods based on boundary integral equations (BIEs), such as the boundary element method (BEM), the boundary face method (BFM) [Zhang JM (2009); F.L. Zhou (2013)]. A near singularity arises when a source point is close to but not on the integration elements. Although those integrals are actually regular in nature, they can't be evaluated accurately by the standard Gaussian quadrature. This is because, the denominator *r*, the distance between the source and the field point, is close to zero but not zero. The difficulty encountered in the numerical evaluation mainly results from the fact that the integrands of nearly singular integrals vary drastically with respect to the distance *r*. Various numerical techniques have been developed to remove the near singularities, such as global regularization [Sladek (1993); Liu (1999)], semi-analytical or analytical integral formulas [Niu (2005); Zhou (2008)], the sinh transformation [Johnston (2005)], polynomial transformation [Tells (1987)], adaptive subdivision method [Gao (2000); Zhang J.M (2009)], distance transformation technique [Ma (2001), (2001); Qin (2011)], the PART method [Hayami (1994), (2005)], and the exponential transformation [Xie (2011); Zhang YM (2009), (2010)]. Most of them benefit from the strategies for computing singular integrals. Among those techniques, the exponential transformation technique seems to be a more promising method for dealing with different orders of nearly singular integrals. However, the transformation is only limited to 2D boundary element and the accuracy is sensitive to the position of the projection point. In this paper, we develop the exponential transformation technique for the nearly singular integrals in 3D boundary element method. Moreover, the improved method is less sensitive to the position of the projection point.

In our method, firstly the conventional distance function is reviewed. Then the conventional distance function is modified into a new form. Based on the modified distance function, the exponential transformation in Refs. [Xie (2011), Zhang YM (2009), (2010)] can be developed to 3D BEM in a new form. Moreover, to perform integrations on irregular elements, the element subdivision technique considering both the element shape and the positions of the project point is employed in combination with the improved transformation. Although the element subdivision technique is used, the computational cost is reduced dramatically compared with the conventional

element subdivision techniques [Gao (2000); Zhang J.M (2009)]. Furthermore, in order to get subtriangles or subquadrangles of good shapes, another nearest point is introduced instead of the projection point when the projection point is located outside the integration element. With our method, the boundary nearly singular integrals of regular or irregular elements can be accurately and effectively calculated. Results demonstrate the accuracy and efficiency of our method. Moreover, our method is less sensitive to the projection of the project point than the conventional exponential transformation method.

This paper is organized as follows. The general form of nearly singular integrals is described in Section 2. Section 3 briefly reviews the distance function in polar coordinate system and then the distance function is constructed in (α, β) coordinate system in a new form. In Section 4, the transformations for nearly singular integrals are presented and the element subdivision technique is introduced. Numerical examples are given in Section 5. The paper ends with conclusions in Section 6.

2. General descriptions

In this section, we will give a general form of the nearly singular integrals over 3D boundary elements. First we consider the boundary integral equations for 3D elasticity problems. The well-known self-regular BIE for elasticity problems in 3-D is

$$0 = \int_{\Gamma} (u_j(\mathbf{s}) - u_j(\mathbf{y})) T_{ij}(\mathbf{s}, \mathbf{y}) d\Gamma - \int_{\Gamma} t_j(\mathbf{s}) U_{ij}(\mathbf{s}, \mathbf{y}) d\Gamma \tag{1}$$

where $\mathbf{s}$ and $\mathbf{y}$ represent the field point and the source point in the BEM, with components s_i and y_i, $i=1,2,3$, respectively and

$$U_{ij} = \frac{1}{16\pi G(1-v)}[(3-4v)\delta_{ij} + r_{,i}r_{,j}]$$

$$T_{ij} = -\frac{1}{8\pi(1-v)}\left\{[\frac{\partial r}{\partial n}(1-2v)\delta_{ij} + r_{,i}r_{,j}] - (1-2v)(r_{,i}n_j - r_{,j}n_i)\right\}$$

Eq. (1) is discretized on the boundary Γ by boundary elements $\Gamma_e(e=1 \sim N)$ defined by interpolation functions. The integral kernels of Eq. (1) become nearly singular when the distance between the source point and integration element is very small compared to the size of integration element. And the integrals in Eq. (1) become nearly singular with different orders, namely,

$U_{ij}(\mathbf{s},\mathbf{y})$ with near weak singularity, and $T_{ij}(\mathbf{s},\mathbf{y})$ with near strong singularity. In this paper, we develop the exponential transformation method for various boundary integrals with near singularities of different orders. The new method is detailed in following sections. For the sake of clarity and brevity, we take following integrals as a general form to discuss:

$$I = \int_S \frac{f(\mathbf{x},\mathbf{y})}{r^l} dS, \quad l = 1,2,3 \quad r = \|\mathbf{x}-\mathbf{y}\|_2 \tag{2}$$

where f is a smooth function, $\mathbf{x}$ and $\mathbf{y}$ represent the field point and the source point in BEM, with components x_i and y_i, respectively. S represents the boundary element. We assume that the source point is close to S, but not on it.

3. Construction of new distance function

3.1 The conventional distance function in polar coordinate

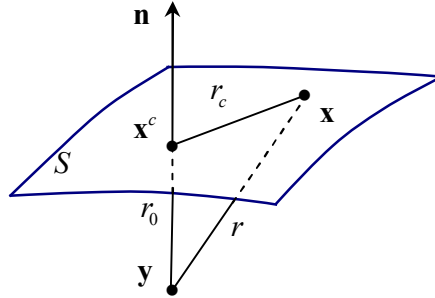In this section, we will briefly review the distance function [Ma (2001), (2001); Qin (2011)].

Figure 1: The minimum distance r_0, from the source point $\mathbf{x^c}$ to the 3D surface element

As shown in Fig.1, employing the first-order Taylor expansion in the neighborhood of the projection point, we have:

$$
\begin{aligned}
x_k - y_k &= x_k - x_k^c + x_k^c - y_k \\
&= \frac{\partial x_k}{\partial t_1}\bigg|_{\substack{t_1=c_1 \\ t_2=c_2}} (t_1 - c_1) + \frac{\partial x_k}{\partial t_2}\bigg|_{\substack{t_1=c_1 \\ t_2=c_2}} (t_2 - c_2) + r_0 n_k(c_1,c_2) + O(\rho^2) \\
&= \rho A_k(\theta) + r_0 n_k(c_1,c_2) + O(\rho^2)
\end{aligned} \tag{3}
$$

where (c_1, c_2) are the coordinates of the projection point in the local system (t_1, t_2), $\rho = \sqrt{(t_1-c_1)^2 + (t_2-c_2)^2}$ and $r_0 = \|\mathbf{x}^c - \mathbf{y}\|$ which is the minimum distance from the source

point to the element in most cases. n_k represents the component of the unit outward direction to the surface boundary and

$$A_k(\theta) = \frac{\partial x_k}{\partial t_1}\bigg|_{\substack{t_1=c_1\\t_2=c_2}} \cos\theta + \frac{\partial x_k}{\partial t_2}\bigg|_{\substack{t_1=c_1\\t_2=c_2}} \sin\theta \tag{4}$$

The distance function is expressed as follows:

$$r^2 = (x_k - y_k)(x_k - y_k) = A_k^2(\theta)\rho^2 + r_0^2 + O(\rho^3) \tag{5a}$$

$$r = \sqrt{A_k^2(\theta)\rho^2 + r_0^2 + O(\rho^3)} \tag{5b}$$

Using Eq. (5a) and Eq. (5b), Eq. (2) can be written as:

$$I = \int_\Gamma \frac{f(\mathbf{x},\mathbf{y})}{r^l} d\Gamma = \sum_m \int_{\theta_m}^{\theta_{m+1}} \int_0^{\rho(\theta)} \frac{g(\rho,\theta)}{(\rho^2 + \omega^2(\theta))^{l/2}} d\rho d\theta \tag{6}$$

where $\omega(\theta) = \dfrac{r_0}{A(\theta)}$, $A(\theta) = \sqrt{A_k(\theta)A_k(\theta)}$, and $g(\rho,\theta)$ is a smooth function.

3.3 Improved distance function in polar coordinate

The conventional distance function has been reviewed in Section 3.1. However, as illustrated in Fig. 2, if the projection point is not the ideal point, the line with end points $\mathbf{x^c}$ and $\mathbf{y}$ is not perpendicular to the tangential plane through $\mathbf{x^c}$.
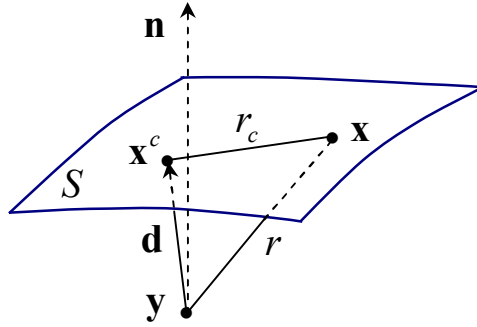

Figure 2: The projection point is not the ideal point

Using Eq. (3) and Eq. (5a), the real distance between the source point and the field points can be written as:

$$r^2 = (x_k - y_k)(x_k - y_k) = a\left[(\rho + \frac{b}{2a})^2 + \frac{r_0^2}{a} - (\frac{b}{2a})^2 + O(\rho^3)\right] \tag{7}$$

where $\quad a = A_k^2(\theta) > 0$, $b = 2d_k A_k(\theta)$, $r_0^2 = |\mathbf{d}|^2$

The following distance function can be given as:

$$r = \sqrt{a}\sqrt{\left[(\rho + \frac{b}{2a})^2 + \delta^2 + O(\rho^3)\right]} \tag{8}$$

where $\quad \delta^2 = \dfrac{r_0^2}{a} - (\dfrac{b}{2a})^2$

With Eq. (7) and Eq. (8), Eq. (2) can be written as:

$$I = \int_\Gamma \frac{f(\mathbf{x}, \mathbf{y})}{r^l} d\Gamma = \sum_m \int_{\theta_m}^{\theta_{m+1}} \int_0^{\rho(\theta)} \frac{g(\rho, \theta)}{\left[(\rho + \dfrac{b}{2a})^2 + \delta^2\right]^{l/2}} d\rho d\theta \tag{9}$$

where $\quad \omega(\theta) = \dfrac{r_0}{A(\theta)}$, $A(\theta) = \sqrt{A_k(\theta)A_k(\theta)}$, and $g(\rho, \theta)$ is a smooth function.

In this section, we obtain the distance function in a new form in the two coordinate systems, respectively. It is should be noted that if the project point is coincide with the ideal projection point, Eq. (9) is similar to Eq. (6). In next section, we will construct the improved exponential transformation based on the refined distance function.

4. Improved transformation and element subdivision technique

4.1 Improved exponential transformation

In this section, we will give the improved transformation considering the modified distance function. As observed from Eq. (6), Eq. (9), the near singularity is essentially related to the radial variable ρ.

Firstly from Eq. (6), we only consider the radial variable integral which depicts near singularity in the Eq. (6), as follows:

$$I_1 = \int_0^{\rho_{max}(\theta)} \frac{g(\rho, \theta)}{(\rho^2 + \omega^2(\theta))^{l/2}} d\rho \tag{7}$$

The following exponential transformation is given as in [Xie, 2013]:

$$\rho = \omega(\theta)(e^{k(1+\eta)} - 1), \ \eta \in [-1,1], \quad k = \ln \sqrt{1 + \rho_{max}/w(\theta)} \tag{8}$$

Using Eq. (8), Eq. (7) can be written as:

$$I_1 = \int_0^{\rho_{\max}(\theta)} \frac{g(\rho,\theta)}{(\rho^2 + \omega^2(\theta))^{l/2}} d\rho = \int_{-1}^1 \frac{k\omega(\theta)e^{k(1+\eta)}g(\rho,\theta)}{\omega^l(\theta)((e^{k(1+\eta)}-1)^2+1)^l} d\eta \tag{9}$$

Eq. (8) is similar to the transformation in Refs. [Xie (2013); Zhang YM (2009), (2010)]. However, for the first time, the exponential transformation is applied for evaluation of nearly singular integrals in 3D elasticity problems.

Then from Eq. (8), the radial variable integral which depicts near singularity in the Eq. (9) is considered, as follows:

$$I_3 = \int_0^{\rho_{\max}(\theta)} \frac{g(\rho,\theta)}{\left[(\rho+\frac{b}{2a})^2+\delta^2\right]^{l/2}} d\rho \tag{10}$$

Using the same steps as in [Xie (2013)], the following exponential transformation is given:

$$\rho = \delta(e^{k(1+\eta)}-1+\frac{b}{2a\delta})-\frac{b}{2a} \quad \eta \in [-1,1], \quad k = \ln\sqrt{1+\rho_{\max}/\delta} \tag{11}$$

Note that if the projection point is the ideal projection point, Eq. (11) is similar to Eq. (8). With the help of the exponential transformation above, the integrals with near weak singularity or near strong singularity can be accurately calculated. It should be noted that we still use the exact r instead of the approximate r in Eq. (2). So the nearly singular kernels are not changed into other forms.

4.2 Exponential transformation in combination with element subdivision

The element subdivision is indispensible for treating the nearly singular integrals in the 3D cases as in Refs. [Ma, 2001; Ma, 2002; Qin, 2011]. In this section, we subdivide an integration element in a suitable pattern considering both element shape and the position of the projection point in the element. Adaptive integration based on element subdivision to calculate integrals is employed just as a combination for the improved exponential transformation. We classify the element subdivision into two cases considering whether the projection point is located in or outside the integration element.

4.2.1 Element subdivision when the projection point is in the integration element

First, we consider the case when the projection point is located in the integration element. Note that although the original quadrangle has a fine shape, the four subtriangles may have poor shapes depending on the position of $\mathbf{x}_c$ (the projection point) (see Fig. 3.(a)). Obtaining triangles of fine shape seems more difficult by direct subdivision for irregular initial elements as shown in Fig. 3(a) even $\mathbf{x}_c$ is located at the element center. If the angle denoted by, Fig. 3(b) – 3(f) between two lines in common with end point $\mathbf{x}_c$ in each triangle is larger by a certain value $2\pi/3$ and even tends to π, numerical results will become less accurate.
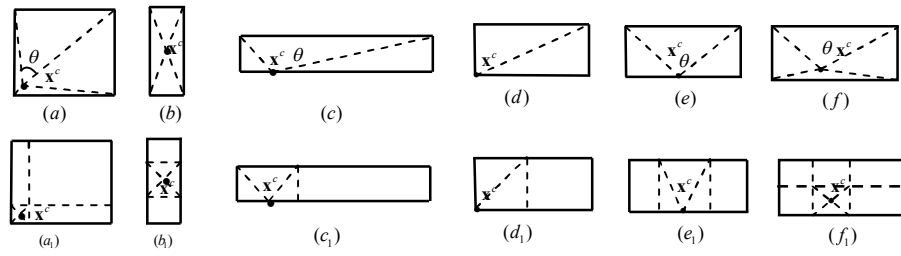

Fig. 3. Subdivisions of quadrilateral element depending on the position of the projection point

To solve the troubles described above, we have developed an adaptive subdivision for an arbitrary quadrilateral element. The original element is divided into several triangles and additional quadrangles, which is different from these as shown in Fig. 3 (*a1*)-(*f1*). The adaptive subdivision consists of three main steps described briefly as follows:

First, compute the distances in the real-world-coordinate system from $\mathbf{x}_c$ to each edge of the element and obtain the minimum distance *d*.

Then, based on *d*, we construct a box defined in parametric system, but with square shape in the real- world -coordinate system as can as possible, to well cover $\mathbf{x}_c$.

Finally, triangles are constructed from the box and additional quadrangles are created outside the box in the element.

Applying the strategy above, adaptive subdivisions for the elements in Fig. 3 with suitable patterns are shown in Fig. 3 (*a1*)-(*f1*). For each triangle, the nearly singular integrals are calculated by the scheme discussed in Section 4.1. However, for each quadrangle, nearly singular integrals will arise but not severe, which can be calculated by adaptive integration scheme based on the element subdivision technique discussed in Refs. [Zhang, 2009]. It should be noted that, although the

element subdivision is adopted, the computational cost is reduced dramatically compared with the conventional subdivision technique to compute nearly singular integrals on the whole element. This is because the integrals on the local region of the element, which is more close to the source point, are calculated by the new variable transformations technique.

Then we consider the case when the projection point is located outside the integration element. Only a few literatures refer to nearly singular integrals of this type, such as the tangential transformation in Ref. [Ma, 2002] and new variable transformations in Ref. [Xie, 2013]. In our implementation, when the projection point is located outside the integration element, another subdivision is employed in our method. The point $\mathbf{x}_d$ which is the most close point to the source point in the element is introduced. The positions of the nearest point are shown in Fig. 4. We subdivide the element in three triangles around $\mathbf{x}_d$ instead of the projection point. And the transformations (11) are employed for nearly singular integrals in each triangle. In this subdivision, the nearest point is always in the element, so we still can follow the three main steps.
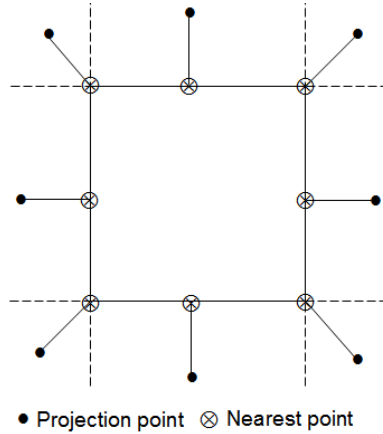

● Projection point ⊗ Nearest point

Fig. 4. The positions of the nearest point

5. NUMERICAL EXAMPLES

Example 1: A regular quadrilateral element to verify the sensitiveness to the position of the projection point

In this example, we study the influence of the projection point on our method when the source point is fixed. Four vertexes of the element locate at (0, 0, 0), (1.0, 0, 0), (1.0, 1.0, 0) and (0, 1.0, 0), respectively. In each case, the source point is fixed at (0.5, 0.5, 0.01), and the projection point **P** is determined by an offset parameter $k, 0 \le k \le 1$, using the following equation :

$$\mathbf{p} = \mathbf{x}^c + k\mathbf{x}^c \qquad (12)$$

Where $\mathbf{x}^c$ is the ideal projection point at the centre of the element with coordinates (0, 0) in local (t_1, t_2) system if we constrain both t_1 and t_2 in [-1, 1].
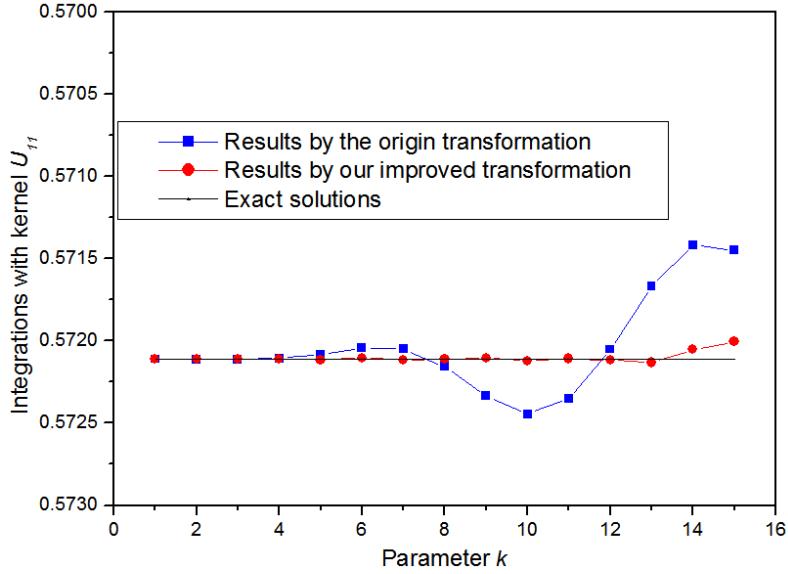

Figure 6:   Various integrals with the kernel U_{11}

Given a set of values of k, all computations have been performed with our method using Eq. (19) and Eq. (23) respectively. The reference values are obtained by adaptive element subdivisions [Zhang J.M (2009)]. As shown in Fig. 6, it is obvious that, the results obtained by Eq. (23) are in good agreement with the reference values even the offset parameter k increases up to 15%, and the maximum error is less than 0.02 percent. The results obtained by Eq. (19) are not as accurate as that of Eq. (23). And the maximum error from Eq. (19) is 1.2 percent within the offset parameter $0 \le k \le 0.15$. As shown in Fig. 7, , the results obtained by Eq. (23) are also in good agreement with the reference values even the offset parameter k increases up to 15%, and the maximum error is less than 0.8 percent, while the maximum error from Eq. (19) is about 8.2 percent within the offset parameter $0 \le k \le 0.15$.
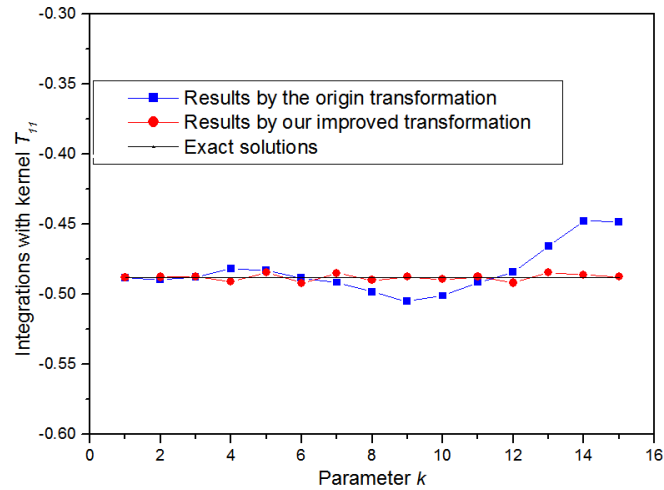
Figure 7: Various integrals with the kernel T_{11}

It is should be noted that although in most cases the projection point coincides with the ideal projection point, the special cases of the offset projection point are also considered in this paper. In our implementation, the improved exponential transformation is applied for evaluation of the nearly singular integrals arising in 3D boundary elements. This is because the accuracy of the results is less sensitive to the position of the project point.

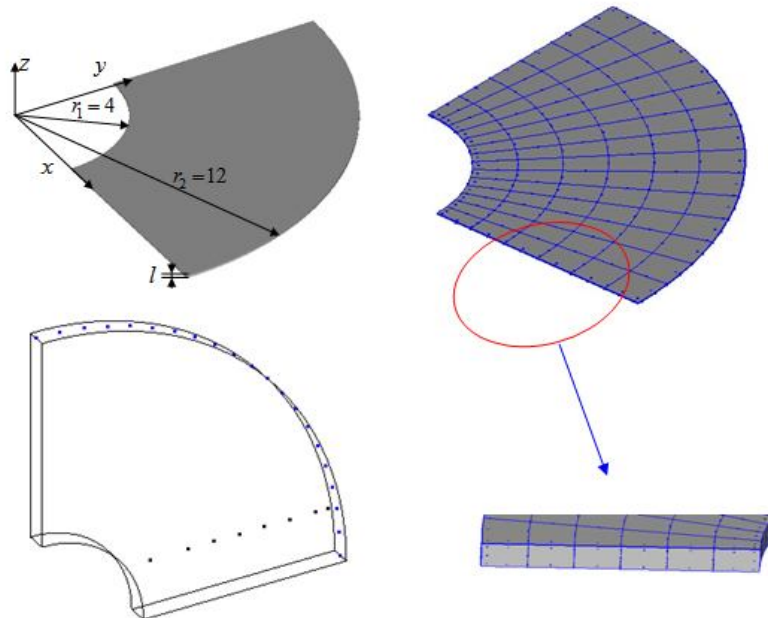***Example 2:   Hollow circular cylinder problems***

Figure 7: Hollow circular cylinder elasticity problem

The first case considers a hollow cylinder elasticity problem. In this case, the geometry, and the BEM model for this problem are shown in Fig. 7. As illustrated in Fig. 7, the elements are slender elements in the side surfaces. To evaluate the nearly singular integrals, the improved

transformation combined with the element subdivision technique is applied. We assume the thickness l is *0.08* or *0.008*. The Young's modulus is 1 and the Poisson's ratio is *0.25*. In order to make comparison with the exact solutions, boundary conditions are imposed on all faces corresponding to quadratic exact solutions. And the solutions are as follows:

$$\begin{cases} u_1 = -2x^2 + 3y^2 + 3z^2 \\ u_2 = 3x^2 - 2y^2 + 3z^2 \\ u_3 = 3x^2 + 3y^2 - 3z^2 \end{cases} \tag{28}$$

As shown in Fig. 7, the BEM model with 179 8-node quadrilateral elements and the total number of nodes is 753. The sample points are distributed on the boundary. The boundary evaluation points are uniformly distributed on isoparametric line segment from (0.0, 0.5) to (1.0, 0.5) in the parametric space of the outer cylinder surface. In this space, $u \in [0,1]$ and $v \in [0,1]$. And the results at the boundary sample points are illustrated in Fig. 8 and Fig. 9. The exact solutions are computed through Eq. (28), and numerical solutions are obtained by BEM using Eq. (26) for nearly singular integrals.
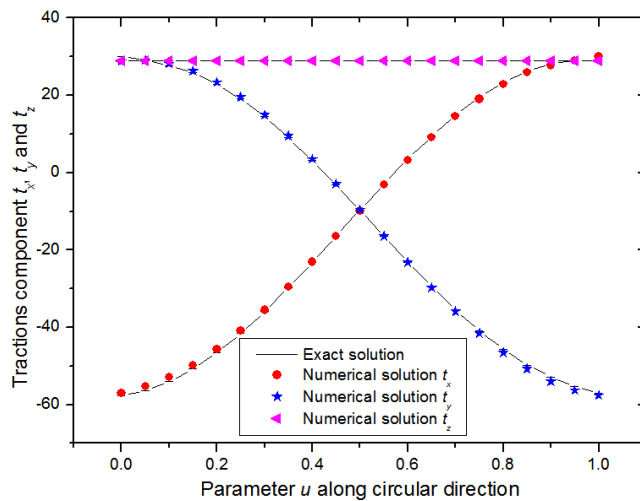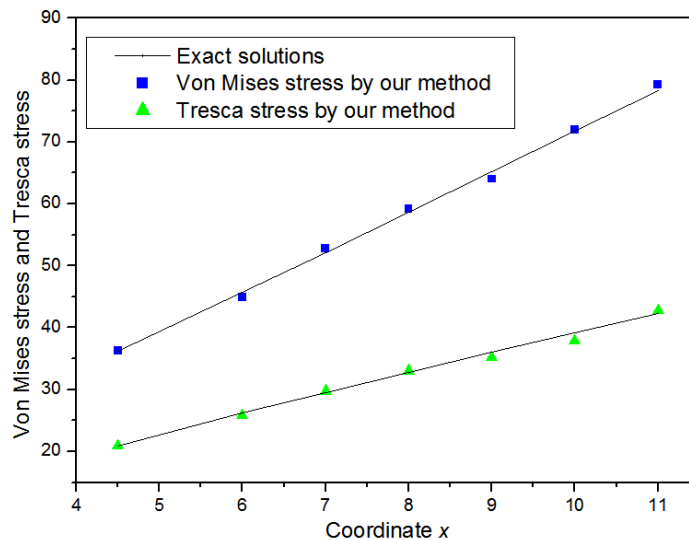

Figure 8:

Results at the
points when

boundary
l=0.08

Results at the
domain points

when l=0.08

Figure 9: Results at the boundary points when l=0.008

As illustrated in Fig. 8 and Fig. 9, the numerical solutions obtained by the proposed method are in good agreement with the exact solutions for the linear elasticity problem. The results of our method keep stable and reasonable accuracy using the model of same meshes. It can be concluded from this example that the proposed method is suitable for linear elasticity problems in thin structures. Note that, the slender element, of which the length and width ratio is larger than 10, is applied for long and narrow surfaces in this example. However, in our method the accuracy is not influenced by elements with poor quality.

Example 3: **Thin cylindrical shell with fixed ends subjected to constant internal pressure**

This problem setup and a radial displacement profile are shown in Fig. 10. Note that the fixed ends create boundary layers which are difficult to capture with finite element methods. The exact shell theory solution is given in Ref. [Hughes (2005)], for plane stress and provided as a reference below:

$$u(x) = -\frac{PR^2}{Et}(1 - C_1 \sin \beta x \sinh \beta x - C_2 \cos \beta x \cosh \beta x) \quad x \in (-L/2, L/2) \qquad (32)$$

where $C_1 = \dfrac{\sin \alpha \cosh \alpha - \cos \alpha \sinh \alpha}{\sinh \alpha \cosh \alpha + \sin \alpha \cos \alpha}$, $C_2 = \dfrac{\cos \alpha \sinh \alpha + \sin \alpha \cosh \alpha}{\sinh \alpha \cosh \alpha + \sin \alpha \cos \alpha}$

The sample points are uniformly distributed on the line segment which has end points at (*-2.01, 0, -4.99*) and (*-2.01, 0, 4.99*). The Young's modulus is *1800* and the Poisson's ratio is *0.25*. The BFM model with *448* 8-node quadrilateral elements and the total number of nodes is *1454*. Results at the sample points are illustrated in Fig. 11.

Figure 10: surface meshes of Thin cylindrical shell, meshes, and the the end face

$R = 2.0$

$t = 0.02$
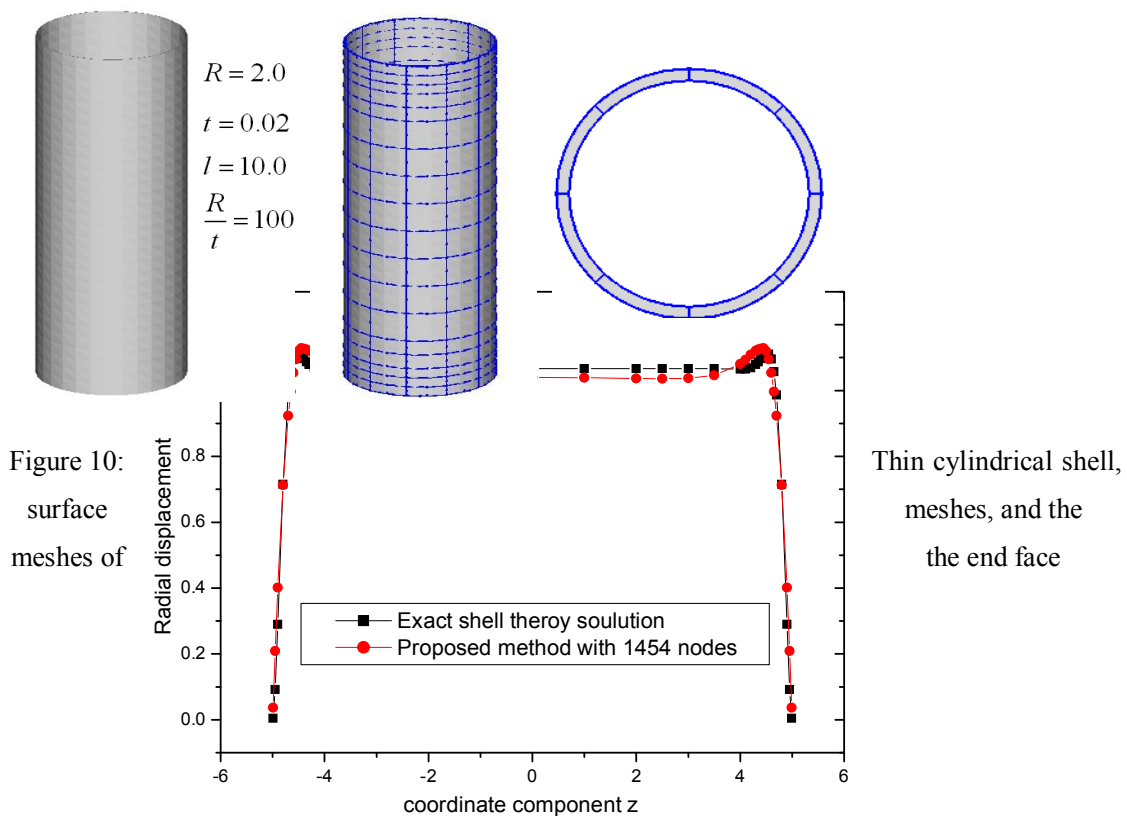
$l = 10.0$

$\dfrac{R}{t} = 100$

Figure 11: Numerical radial displacement compared with the shell theory solution

From Fig. 11, although the results are not that accurate, it can be seen that the numerical radial displacement profile captures the boundary layers and picks up the plateau very well. Compared with FEM, the plate and shell theories based on various assumptions about the geometry are not needed in BEM. Moreover, compared with the method in [Hughes (2005)], no solid element is required in BEM.

6. CONCLUSIONS

This paper presented an improved exponential transformation for nearly singular integrals which appears in the application of BEM for elasticity problems. By applying the proposed transformation in the BEM, the number of integral points in the near singular integral patches has been reduced significantly. Furthermore, results obtained by the proposed method are less sensitive to the location of the projection point than that obtained by traditional exponential transformation method.

To perform integration on irregular elements, an adaptive integration scheme considering the element shape and the projection point in combination with the improved transformation has been introduced. Numerical examples have been presented to verify the proposed method. Results demonstrate the accuracy and efficiency of our method. The sensitivity of the results to the position of the projection point has also been demonstrated. For nearly hypersingular integrals or other nearly singular integrals of higher orders, however, the present method is not so effective. Extending our method to compute nearly hypersingular integrals is ongoing.

REFERENCES

Aliabadi, M.H.; Martin, D. (2000): Boundary element hypersingular formulation for elastoplastic contact problems. *International Journal for Numerical Methods in Engineering*, vol. 48, no. 7, pp. 995-1014.

Johnston, B. M.; Johnston, P. R.; Elliott, D. (2007): A sinh transformation for evaluating two‐dimensional nearly singular boundary element integrals. *International journal for numerical methods in engineering*, vol. 69, no.7, pp. 1460-1479.

Cruse, T. A.; Aithal, R. (1993): Non-singular boundary integral equation implementation. *International journal for numerical methods in engineering*, vol. 36, no. 2, pp. 237-254.

Chen, H. B.; Lu, P.; Huang, M. G.; Williams, F. W. (1998): An effective method for finding values on and near boundaries in the elastic BEM. *Computers & structures*, vol. 69, no. 4, pp. 421-431.

Dirgantara, T.; Aliabadi, M. H. (2000): Crack growth analysis of plates loaded by bending and tension using dual boundary element method. *International journal of fracture*, vol. 105, no. 1, pp. 27-47.

F.L. Zhou.; G.Z. Xie.; J.M. Zhang.; X.S. Zheng. (2013): Transient heat conduction analysis of solids with small open-ended tubular cavities by boundary face method. *Engineering Analysis with Boundary Elements*, vol. 37, no. 3, pp. 542-550.

Gao, X. W.; Davies, T. G. (2000): Adaptive integration in elasto-plastic boundary element analysis. *Journal of the Chinese institute of engineers*, vol. 23, no .3, pp. 349-356.

Hayami, K.; Matsumoto, H. (1994): A numerical quadrature for nearly singular boundary element integrals. *Engineering Analysis with Boundary Elements*, vol.13, no. 2, pp. 143-154.

Hayami, K. (2005): Variable transformations for nearly singular integrals in the boundary element method. *Publications of the Research Institute for Mathematical Sciences*, vol. 41, no. 4, pp. 821-842.

Hughes, T. J.; Cottrell, J. A.; Bazilevs, Y. (2005): Isogeometric analysis: CAD, finite elements, NURBS, exact geometry and mesh refinement. *Computer methods in applied mechanics and engineering*, vol. 194, no. 39, pp. 4135-4195.

Johnston, P. R.; Elliott, D. (2005): A sinh transformation for evaluating nearly singular boundary element integrals. *International journal for numerical methods in engineering*, vol. 62, no. 4, pp. 564-578.

Krishnasamy, G.; Rizzo, F. J.; Liu, Y. (1994): Boundary integral equations for thin bodies. *International Journal for Numerical Methods in Engineering*, vol. 37, no. 1, pp. 107-121.

Liu, Y. J. (1998): Analysis of shell-like structures by the boundary element method based on 3-D elasticity: formulation and verification. *International Journal for Numerical Methods in Engineering*, vol. 41, no. 3, pp. 541-558.

Liu, Y. J.; Rudolphi, T. J. (1999): New identities for fundamental solutions and their applications to non-singular boundary element formulations. *Computational mechanics*, vol. 24, no. 4, pp. 286-292.

Ma, H.; Kamiya, N. (2002): A general algorithm for the numerical evaluation of nearly singular boundary integrals of various orders for two-and three-dimensional elasticity. *Computational Mechanics*, vol. 29, no. 4, pp. 277-288.

Ma, H.; Kamiya, N. (2001): A general algorithm for accurate computation of field variables and its derivatives near the boundary in BEM. *Engineering analysis with boundary elements*, vol. 25, no. 10, pp. 833-841.

Ma, H.; Kamiya, N. (2002): Distance transformation for the numerical evaluation of near singular boundary integrals with various kernels in boundary element method. *Engineering analysis with boundary elements*, vol. 26, no. 4, pp. 329-339.

Niu, Z.; Wendland, W. L.; Wang, X.; Zhou, H. (2005): A semi-analytical algorithm for the evaluation of the nearly singular integrals in three-dimensional boundary element methods. *Computer methods in applied mechanics and engineering*, vol. 194, no. 9, pp. 1057-1074.

Qin, X.; Zhang, J.; Xie, G.; Zhou, F.; Li, G. (2011). A general algorithm for the numerical evaluation of nearly singular integrals on 3D boundary element. *Journal of computational and applied mathematics*, vol. 235, no. 14, pp. 4174-4186.

Sladek, V.; Sladek, J.; Tanaka, M. (1993): Regularization of hypersingular and nearly singular integrals in the potential theory and elasticity. *International Journal for Numerical Methods in Engineering*, vol. 36, no. 10, pp. 1609-1628.

Tells,J.C.F. (1987): A self adaptive coordinate transformation for efficient numerical evaluations

of general boundary element integrals, *International Journal for Numerical Methods in Engineering*, vol. 24, no. 5, pp. 959-973.

Xie, G.; Zhang, J.; Qin, X.; Li, G. (2011): New variable transformations for evaluating nearly singular integrals in 2D boundary element method. *Engineering Analysis with Boundary Elements*, vol. 35, no. 6, pp. 811-817.

Zhang, D.; Rizzo, F. J.; Rudolphi, Y. J. (1999): Stress intensity sensitivities via hypersingular boundary element integral equations. *Computational Mechanics*, vol. 23, pp. 389-396.

Zhou, H.; Niu, Z.; Cheng, C.; Guan, Z. (2008)：Analytical integral algorithm applied to boundary layer effect and thin body effect in BEM for anisotropic potential problems. *Computers & Structures*, vol. 86, no. 15, pp. 1656-1671.

Zhang JM.; Qin XY.; Han X.; Li GY.(2009): A boundary face method for potential problems in three dimensions. *International Journal for Numerical Methods in Engineering*, vol 80, no.3, pp. 320–337.

Zhang YM.; Gu Y,; Chen JT. (2009): Boundary layer effect in BEM with high order geometry elements using transformation. *CMES- Computer Modeling in Engineering and Sciences*, vol. 45, no. 3, pp. 227-247.

Zhang, Y.; Gu, Y.; Chen, J. T. (2010): Boundary element analysis of the thermal behaviour in thin-coated cutting tools. *Engineering Analysis with Boundary Elements*, vol. 34, no. 9, pp. 775-784**.**

算例：U11

0.57211029491803056

0.505 0.57211028637147776	0.57211036901628887
0.510 0.57211185654307661	0.57210968973263132
0.515 0.57211264392269823	0.57211052785914596
0.520 0.57210514421112413	0.57210955277031661
0.525 0.57208181167152972	0.57211407093085020
0.530 0.57204445831515127	0.57210406614085452
0.535 0.57204813455902337	0.57211409584041906

0.540 0.57215606888491910   0.57211121515046381

0.545 0.57233399773121674   0.57210374791021834

0.550 0.57244398940083319   0.57212044160205200

0.555 0.57235341478914969   0.57210712244365969

0.560 0.57205115773492332   0.57211689859940518

0.565 0.57166761814535272   0.57213073076062670

0.570 0.57141596327362187   0.57205295418881819

0.575 0.57144702333587394   0.57200397146528226

算例：T11

-0.48799878246338113

0.505 -0.48796043577992865   -0.48804682319555520

0.510 -0.48908460996366560   -0.48754681974653097

0.515 -0.48775519166118991   -0.48728640488663300

0.520 -0.48160861798152710   -0.49067325888027108

0.525 -0.48285701695827016   -0.48404297802904978

0.530 -0.48832360911452677   -0.49192864073669423

0.535 -0.49143450984193265   -0.48486063122443113

0.540 -0.49816756344362495   -0.48983991283190759

0.545 -0.50495528702176395   -0.48747560027027942

0.550 -0.50094088449720342   -0.48927211074133653

0.555 -0.49136497184879374   -0.48735526680684466

0.560 -0.48394501689511182   -0.49166198658242105

0.565 -0.46528139962593323   -0.48446513312203587

0.570 -0.44753946037457681   -0.48606537406997530

0.575 -0.44833674600284085   -0.48745484324289562

0.580